Advanced Control and Optimization Techniques for Grid-Connected Wind Energy Systems Based on MPPT and Hybrid Controllers.

Gurunandan P H
Department of EEE
SSIT
Tumkur, India

Dr. Shilpa G N
Department of EEE
SSIT
Tumkur, India

Dr. Nataraja C
Department of EEE
SSIT
Tumkur, India

C R Mohan Kumar
Department of ECE
SSIT
Tumkur, India

Praveen M
Department of ECE
SSIT
Tumkur, India

Simha D K L N
Department of ECE
SSIT
Tumkur, India

***Abstract*---The growing integration of renewable energy sources (RES) into power grids is vital for addressing climate change and pollution. Wind energy, in particular, has emerged as a reliable and sustainable option, but its intermittent nature demands effective control strategies to ensure stable operation and improved power quality. This thesis focuses on a grid-connected wind energy conversion system (WECS) using a six-phase permanent magnet synchronous generator (PMSG) with a back-to-back converter topology. The Machine Side Converter (MSC) regulates generator speed, while the Grid Side Converter (GSC) maintains unity power factor and stabilizes the DC link voltage. Incremental conductance (IC)-based Maximum Power Point Tracking (MPPT) is employed to optimize energy capture across varying wind conditions. A detailed WECS model is developed to evaluate different controllers: PI controller and hybrid methods—series PI–Fuzzy and parallel PI–Fuzzy. Their performance is assessed in terms of voltage regulation, frequency stability, harmonic reduction, and robustness under wind and grid variations. Comparative analysis shows that while PI provides satisfactory control, hybrid PI–Fuzzy improves adaptability, offer enhanced robustness under nonlinear conditions. The study contributes practical insights for reliable wind energy integration into modern power grids.**

I. INTRODUCTION

Wind Turbine Generators (WTG) are designed to capture energy from the intermittent wind, which leads to fluctuations in mechanical torque and electrical output, causing voltage variations and power quality (PQ) issues like sag, swell, flicker, and harmonics in the power system as explained by Jabir M et al., 2017, [1]. Variable speed WTGs have gained popularity for their ability to maximize power extraction while minimizing mechanical stress compared to fixed-speed turbines. However, these variable speed systems rely on power electronic converters, which can introduce harmonic distortion into the grid, further exacerbating PQ concerns, proposed by Mohod S W et al., 2010, [2], Thiringer T et al., 2001, [3].

To facilitate the smooth integration of Wind Power Plants (WPP) into the grid and ensure harmonic distortions remain within acceptable limits for utilities and consumers, new standards and grid codes have been developed. Two main approaches, passive and active filtering, are employed to address this issue, Mohamed M A et al., 2016, [4]. Chen Z et al., 2001, have clearly shown that conventional passive filters, consisting of inductors, resistors, and capacitors, are cost-effective and effective at attenuating harmonic components [4]. On the other hand, active filters, though more commonly used, are complex and expensive, particularly at medium and high voltage levels, British Standards Institution, 2007, [5].

Hybrid filters, as defined by International Standard IEC 61400-21, offer a solution that combines the advantages of both active and passive filters in their design. They are capable of providing superior performance in mitigating harmonic resonance issues within WPP [6].

Voltage variation refers to deviations from the normal sinusoidal voltage waveform in a power system network. When integrating Wind Turbines (WT) into the grid, it's crucial to ensure that grid voltage remains within an acceptable range. European voltage standard EN 50160, for example, defines an acceptable range of 10% deviation from the 10-minute average voltages at the end-user level, ensuring that household appliances are not damaged or disrupted as presented by Nassif A B et al., 2007, [7].

IEC Standard 61400-21 specifies that the 10-minute average of voltage fluctuation should be within 5% of its nominal value for the entire wind power plant system which is studied and proposed by Salam Z et al., 2006, [8] and Das J, 2004, [9]. To address the challenges associated with WECS, including power fluctuations, grid integration, and dynamic response, various control strategies have been developed. These strategies play a critical role in ensuring the reliability and stability of the grid when integrating RES like wind power.

One commonly used control strategy is the pitch control, which involves adjusting the pitch angle of the wind turbine blades to regulate the rotational speed and power output. This strategy allows for the limitation of excessive power generation during high wind speeds and the maximization of power capture during low wind speeds. Pitch control helps in maintaining a stable and consistent power output, thus contributing to grid stability. Another widely implemented control strategy is the torque control. By regulating the torque applied to the wind turbine rotor, the

generator's rotational speed and power output can be controlled. Torque control is particularly effective in variable speed WECS, as it allows for optimized power capture under varying wind conditions. Additionally, it aids in minimizing mechanical stress on the turbine components and enhancing overall system reliability. In recent years, advanced control strategies based on model predictive control (MPC) and adaptive control have gained attention in WECS research. MPC utilizes mathematical models and predictive algorithms to optimize control actions and achieve desired system performance. It takes into account various factors, including wind speed, generator characteristics, and grid requirements, to determine the optimal control inputs in real-time. This approach offers enhanced system efficiency and improved response to changing operating conditions. Adaptive control strategies aim to continuously adjust control parameters based on system feedback and external conditions. These strategies enable the system to adapt to changing wind conditions and system dynamics, improving overall performance and stability. Adaptive control techniques, such as fuzzy logic control and neural networks have shown promise in enhancing the control of WECS under different operating conditions. Furthermore, grid integration and power quality control strategies are crucial for ensuring the seamless integration of WECS into the power grid. These strategies involve monitoring and regulating the power flow, voltage, and frequency to comply with grid codes and maintain grid stability. Various control techniques, including active and reactive power control, voltage regulation, and grid synchronization, are employed to achieve optimal grid integration and power quality. Overall, the investigation of existing control strategies in WECS focuses on optimizing power capture, enhancing system stability, and ensuring grid compatibility. The selection and implementation of appropriate control strategies depend on factors such as turbine type, wind conditions, grid requirements, and system objectives. Ongoing research and development continue to explore advanced control techniques to further improve the performance and efficiency of WECS in the rapidly evolving renewable energy landscape.

Integration of converter with variable speed WECS is a challenging task. During the generation of references, frequency, phase, and amplitude of the voltage contributes maximum. Precise estimation of frequency during disturbed voltage is of paramount importance. 3-ϕ PLL is the key element for frequency and phase estimation of the power system voltage. Various PLL schemes are presented in by Saeed Golestan et al., 2017, [10] and SRF-PLL is mostly used one as it is simpler. Its use is restricted due to ripples during measurement of disturbed voltage. Advanced PLL, with additional filters in the conventional SRF-PLL are able to enhance the capability of rejecting the disturbance. Adaptive frequency estimation loop based SRF-PLL as stated and implemented by M Karimi-Ghartemani et al., 2012, [11] is able to eliminate ripples in voltage during frequency variations.

Notch filter (NF)-PLL makes the signals to stay within a band and cancels unwanted harmonics. NF-PLL is associated with high computation. MAF based PLL possess the improved filtering capability presented by S Golestan et al., 2014, [12] and can block specific frequency signals with low cost of computation and effectiveness during disturbance. MAF-PLL shows the slow dynamic response and is shown by Zunaib Alia et al., 2018, [13]. Enhanced MAF-PLL is presented in the literature by Vineet P Chandranh et al., 2019, [14] for PMSG based hydro system, which eliminates frequency-ripples of even orders. Offset rejection method using DSOGI-PLL is presented in the research work by Md. Shamim Reza et al., 2012, [15]. For finding the orthogonal-signals, DSOGI is better substitute of Clarke's transformation. DSOGI-PLL offers no delay in filtering and simple implementation. Under faulty conditions, characteristics of fast frequency adaption is observed and proposed by Pedro Rodriguez et al., 2012, [16].

Harrag A & Messalti S, 2015, have applied GA-based Proportional Integral Derivative (PID) controller to present a best altered PO MPPT algorithm with adjustable duty cycle phase. Because of its simplicity, MPPT algorithm and the classical PO had been commonly used in various applications; however, PO is susceptible to non-success, particularly when elevated irradiance changes, oscillation around the maximum power point and intersect velocity. A technique based on the changeable-step size of altered PO MPPT technique using PID controller tuned by genetic algorithm is provided to address this challenge and to overcome the disadvantages of the classical PO MPPT [17].

Linus R M & Damodharan P, 2015, have analysed the performance of MPPT in grid connected PMSG based WECS. The performance using linear interconnection between ideal speed and velocity of wind was examined. Back-to-back sinusoidal pulse width modulation scheme was presented in the system. The grid side inverter played a significant part in the transfer of produced wind energy from DC-link to the grid and the DC connection voltage regulation [18].

Fesharaki V J et al., 2018, provided a solid and restriction linearization device FLC with altered Incremental Conductance (IC) for MPPT in photovoltaic systems, and the inner consistency of the general closed loop was ensured. The suggested load-related method was autonomous and robust against voltage of load disturbances. At the foundational operational level, a boost chopper converter served as the interface between the Photo Voltaic (PV) panel and the load to govern the system. An adapted Incremental Conductance (IC) technique, based on existing non-division equations, was implemented. The IC technique was employed to initiate the desired current for the Fuzzy Logic Controller (FLC). The FLC swiftly steered the PV panel to its maximum power point while adhering to the constraints of the control duty cycle [19]. The presented speed algorithm was validated experimentally. Additionally, this study delved into the application of PI controllers and Fuzzy Logic Controllers (FLC), both individually and in combination with the standard PI controller, to regulate rotor velocity, reactive power, active power, and dc-link voltage. Notably, gain detection was considered, with the first controller acting as a gain tuner for the second one [20].

Asghar A B & Liu X, 2018, introduced a centered on hybrid intelligent training for the online estimation of wind turbine efficient wind speed using instantaneous wind turbine tip speed ratio, rotor velocity, and mechanical energy. They utilized a hybrid optimization technique to adjust the parameters of the fuzzy Membership Function (MF) in an Artificial Neural Network (ANN). Furthermore, they applied

the estimated efficient wind speed to develop an optimal rotor velocity estimator for variable-speed Wind Turbines (WT) to maximize Power Point Tracking (MPPT). For standalone WECS, variation in load and wind velocity leads to oscillations in the terminal voltage and frequency. The oscillations in the load side terminal voltage need to be reduced for better management of power. For standalone WECS, bi-directional VSC can convert variable voltage into a constant voltage output. Operation of the VSC can be controlled using a PI controller. Due to simple design & implementation, IOPID controllers are used mostly. But, IOPI shows sensitivity towards system's parameters & non-linarites and weaker disturbance rejection with poor transient response [21]. As compared to IOPI, FOPI offers reduction in % THD, response time, overshoot, oscillation, and improvement in transient action, Deepak Pullaguram et al., 2018, [22].

For maximum power extraction, power factor improvement, FOPI are utilized for grid connected PMSG as introduced by Beddar Antar et al., 2015, [23]. FOPI controller enhances the dynamic performance of variable speed WECS in comparison to IOPI and fuzzy controls that is presented by C Vivierors et al., 2014, [24]. System's nonlinearity and wind variation cause PI and FOPI based methods to not provide significant response and show lesser robustness under disturbances and uncertain parameters. Therefore, focus has been to develop nonlinear controls. Robust and adaptive controls are utilized for performance enhancement of WECS. In classical PID, ensuring good performances with disparate plants and guaranteeing a suitable adaptation for time dependent plant is difficult. SMC based robust control shows effective performance, high accuracy & efficiency, stability under uncertainties and system disturbances. SMC makes the response to converge to a sliding surface which is defined in advance and force it to stay on this surface, Y Soufi et al., 2016, [25].

Mao Jingfeng et al., 2015, introduced to SMC showing robustness against the variation in load under unstructured uncertainties in PMSG based WECS. Model uncertainties and disturbances restrict the effectiveness of these model based control strategies. Complex mathematical modeling of partially known or unknown systems is removed in Model Free Control (MFC) incurring low computational cost. MFC provides smooth control variable and is more robust with respect to noises, but a noise signal's derivation is required for SMC. Intelligent PI (iPI) and iPID controllers are the more recent development for the systems with significant model uncertainty and disturbances. In iPID controllers, without any modeling and identification procedure, strongly nonlinear and time dependent system's unknown dynamics is considered and displays better efficiency and response as compared to conventional PID [26]. For control of the systems with high nonlinearities, iPID-MFC is found appropriate as proved and explained by L Sidhom et al., 2016, [27]. A design and stability analysis of iPI-MFC based controller with better trajectory tracking performance is presented by Y Feng et al., 2002, [28].

Transient swings in the manipulator during tracking of train of pulses are reduced and external disturbances are handled using iPI. Also, noise from the manipulator's dynamics is removed. Two model free SMC techniques for control of tracking error dynamics of aerodynamic system are presented by Radu-Emil Precup et al., 2017, [29] and compared with a model free iPI controller. These schemes show robustness against the disturbances and variations in parameters.

Design of Integral-SMC for PMSG based WECS is illustrated by Rachid Errouissi & Ahmed Al-Durra, 2018, [30]. This control includes the reference jump and allows it to achieve nominal performance recovery under uncertainty in model. This control provides satisfactory reference command tracking. In SMC, extra integral term for state variable suppress the SSE provides robustness against the large oscillations in load and system parameter in comparison to classical integral SMC. The robustness of DISMC against uncertainties is verified for WT for lesser than rated wind velocity. A DISMC is utilized and explained clearly by Yoon-Cheul Jeung & Dong-Choon Lee, 2019, [31] for bi-directional dual active bridge DC-DC converter. With DISMC, SSE and chattering are suppressed with fast response under transient. The conventional SMC provides more chattering. TSMC offers robustness to the system against uncertainties by avoiding high-frequency-switching. Conventional TSMC exhibits precision and quick response, but convergence is slow. To suppress these flaws, Non-singular TSMC is presented by Kaihui Zhao et al., 2019, [32].

A robust NSTSMC is discussed by Y Feng et al., 2002 for enhancement of response, fault tolerance, and tracking accuracy of PMSM irrespective disturbances and of demagnetisation of PM [33]. Integral TSMC is proposed by Mohammad Javad Morshed & Afef Fekih, 2019, for improvement chattering and power quality during unbalance in voltage [34]. A non-singular fast TSMC (NFTSMC) with devoid of chattering is discussed in detail by Zhenxin He et al., 2014 for improved tracking-precision [35].

Six-Phase Synchronous Machines: Schiferl RF's work in 1983 included a comprehensive circuit diagram of a six-phase synchronous machine, considering mutual leakage couplings between two sets of three-phase stator windings. Different modes of power transfer and practical winding configurations were examined, particularly in the context of uninterruptible power supply systems [36]. A recent research, carried out by Nataraja and Dr. G. S. Sheshadri, focuses on the intelligent control of six-phase Permanent Magnet Synchronous Generator (PMSG) in grid-connected WECS. This work likely involves advanced control strategies and modeling techniques to optimize the performance of PMSG in wind energy applications [37]. Artificial Neural Networks (ANN) and Fuzzy Logic (FL): The references highlight the advantages of both ANN and FL in control and decision-making processes. ANN is known for its strong numerical learning capabilities, while FL offers interpretability and the integration of expert knowledge. The hybridization of ANN and FL, known as Adaptive Neuro-Fuzzy Inference Systems (), combines the learning capabilities of ANN with the interpretability of FL, making it a powerful tool for control and modeling. Neuro-Fuzzy Systems in Smart Grids: The application of neuro-fuzzy systems in smart grid technology is emphasized. These systems are used to control real-time parameters of the operating system in smart grids. The integration of neural networks with fuzzy logic has the potential to significantly enhance power system efficiency and performance [38-45].

Different literature in the previous researches has given advanced intelligent methods to control the wind energy systems. This paper attempts to improve the performances of the controllers using hybrid methods that would combine the model adaptability with traditional controllers and higher dynamics due to intelligent methods. Thus the combination of the traditional method and the expert systems is considered for the implementation thus carried out to check the performance enhancement of the wind energy conversion systems. The six phase generators are used in the implementation with the hybrid controllers that combine PI controllers and Fuzzy Logic Controllers to enhance the performance of power delivery in the Wind Energy conversion system.

II. METHODOLOGY

This generator is considered a non-salient pole machine. This means that it doesn't have pronounced salient poles or protrusions in its structure. Additionally, the direct and quadrature inductances of the machine are set to equal values, simplifying its analysis and control.Modeling of six-phase synchronous machine is derived from equation, the flux linkage, DQ transformation and current generated are given below.

Flux linkages of six-phase synchronous machine

$$\Psi_{q1} = \omega_{eb}\int V_{q1} - \omega\Psi_{d1} + \frac{R_s}{L_{l2}}(\Psi_{mq} - \Psi_{q1}) \quad (1)$$

$$\Psi_{q2} = \omega_{eb}\int V_{q2} - \omega\Psi_{d2} + \frac{R_s}{L_{l2}}(\Psi_{mq} - \Psi_{q2}) \quad (2)$$

$$\Psi_{d1} = \omega_{eb}\int V_{d1} - \omega\Psi_{q1} + \frac{R_s}{L_{l1}}(\Psi_{md} - \Psi_{d1}) \quad (3)$$

$$\Psi_{d2} = \omega_{eb}\int V_{d2} - \omega\Psi_{q2} + \frac{R_s}{L_{l2}}(\Psi_{md} - \Psi_{d2}) \quad (4)$$

$$\Psi_{kq} = \omega_{eb}\int V_{kq} + \frac{R_{kg}}{L_{kg}}(\Psi_{mq} - \Psi_{kq}) \quad (5)$$

$$\Psi_{kd} = \omega_{eb}\int V_{kd} + \frac{R_{kd}}{L_{kd}}(\Psi_{md} - \Psi_{kd}) \quad (6)$$

$$\Psi_{fd} = \omega_{eb}\int V_{fd} + \frac{R_f}{L_{lfd}}(\Psi_{md} - \Psi_{fd}) \quad (7)$$

$$\Psi_{mq} = \frac{L_{ag}}{L_{l1}}\Psi_{q1} + \frac{L_{ag}}{L_{l2}}\Psi_{q2} + \frac{L_{ag}}{L_{lkg}}\Psi_{kq} \quad (8)$$

$$\Psi_{md} = \frac{L_{ad}}{L_{l1}}\Psi_{d1} + \frac{L_{ad}}{L_{l2}}\Psi_{d2} + \frac{L_{ad}}{L_{lfd}}\Psi_{fd} + \frac{L_{ad}}{L_{kd}}\Psi_{kd} \quad (9)$$

Current equations

$$I_{q1} = -\frac{1}{L_{l1}}(\Psi_{q1} - \Psi_{mq}) \quad (10)$$

$$I_{d1} = -\frac{1}{L_{l1}}(\Psi_{d1} - \Psi_{md}) \quad (11)$$

$$I_{kq} = -\frac{1}{L_{lkg}}(\Psi_{kq} - \Psi_{mq}) \quad (12)$$

$$I_{fd} = \frac{1}{L_{lfd}}(\Psi_{fd} - \Psi_{md}) \quad (13)$$

$$I_{q1} = -\frac{1}{L_{l2}}(\Psi_{q2} - \Psi_{mq}) \quad (14)$$

$$I_{d2} = -\frac{1}{L_{l2}}(\Psi_{d2} - \Psi_{md}) \quad (15)$$

$$I_{kd} = -\frac{1}{L_{lkd}}(\Psi_{kd} - \Psi_{md}) \quad (16)$$

ABC to DQO transformation of Voltage

Let

$$p = \frac{2V_a + 2V_b}{3} \quad (17)$$

$$q = \frac{-V_a - V_b}{3} \quad (18)$$

$$r = \frac{-V_a + 2V_b}{3} \quad (19)$$

$$s = \frac{2V_x + V_y}{3} \quad (20)$$

$$t = \frac{-V_x - V_y}{3} \quad (21)$$

$$u = \frac{-V_x + 2V_y}{3} \quad (22)$$

$$V_{q1} = \frac{2}{3}[p\cos(\theta) + q\cos(\theta - \frac{2\pi}{3}) + r\cos(\theta + \frac{2\pi}{3}) \quad (23)$$

$$V_{d1} = \frac{2}{3}[p\sin(\theta) + q\sin(\theta - \frac{2\pi}{3}) + r\sin(\theta + \frac{2\pi}{3}) \quad (24)$$

$$V_{q2} = \frac{2}{3}[s\cos(\theta - \delta) + t\cos(\theta - \frac{2\pi}{3} - \delta) + u\cos(\theta + \frac{2\pi}{3} - \delta) \quad (25)$$

$$V_{q1} = \frac{2}{3}[s\sin(\theta - \delta) + t\sin(\theta - \frac{2\pi}{3} - \delta) + u\cos(\theta + \frac{2\pi}{3} - \delta) \quad (26)$$

ABC to DQO transformation of Current

$$I_a = I_{q1}\cos(\theta) + I_{d1}\sin(\theta) \quad (27)$$

$$I_b = I_{q1}\cos(\theta - \frac{2\pi}{3}) + I_{d1}\sin(\theta - \frac{2\pi}{3}) \quad (28)$$

$$I_c = -I_a - I_b \quad (29)$$

$$I_x = I_{q2}\cos(\theta - \delta) + I_{d2}\sin(\theta - \delta) \quad (30)$$

$$I_y = I_{q2}\cos(\theta - \frac{2\pi}{3} - \delta) + I_{d2}\sin(\theta - \frac{2\pi}{3} - \delta) \quad (31)$$

$$I_z = -I_x - I_y \quad (32)$$

- Ψ_{q1}, Ψ_{q2} - quadrature axis flux linkage in abc (1) and xyz (2) windings respectively
- Ψ_{d1}, Ψ_{d2} - quadrature axis flux linkage in abc (1) and xyz (2) windings respectivel
- Ψ_{kd}, Ψ_{kq} - direct and quadrature axis flux linkage in damper windings
- Ψ_{fd} - flux linkage in field windings
- Ψ_{md}, Ψ_{mq} - direct and quadrature axis mutual flux
- I_{d1}, I_{d2} - direct axis flux current in abc (1) and xyz (2) windings respectively
- I_{q1}, I_{q2} - quadrature axis current in abc (1) and xyz (2) windings respectively
- I_{fd} - direct axis current in field windings
- I_{kd}, I_{kq} - direct and quadrature axis current in damper windings
- V_{d1}, I_{d2} - direct axis voltage in abc (1) and xyz (2) windings respectively
- V_{q1}, I_{q2} - quadrature axis voltage in abc (1) and xyz (2) windings respectively
- V_{fd} - direct axis voltage in field windings
- V_{kd}, I_{kq} - direct and quadrature axis voltage in damper windings
- θ - system frequency in hz (πft)
- ω,δ - the angular difference between abc and xyz phase, here it is 30°
- ω_{eb} - Electrical base angular velocity
- R_s - Resistance of stator winding, R_f - Resistance of field winding

L_{l1}, L_{l2} - Leakage field inductance of field winding

L_{kd}, L_{kq} - Self-inductance of direct and quadrature axis in damper winding

R_{kd}, R_k - Resistance of direct and quadrature axis in damper winding

III. CONTROLLER REQUIREMENTS FOR POWER QUALITY ENHANCEMENT

Considering the friction and the size constraints involved in the geared WECS the gearless WECS is considered in the research implementation. The gearless setup leads to the VSWECS, and with PMSG involved in the research higher number of poles is involved as discussed previously in this thesis. Higher number of poles introduces harmonics in the generator and thus a portion of the power generated would contribute to the reactive power loss. A control technique along with the converter that limits the harmonics in the generator output assures usable power delivery. The geared WECS with induction generators is inherent with disadvantages like reactive power consumption, poor power quality, and mechanical stress. Grid voltage fluctuations due to gear control for maintaining constant speed output at the generator is considered as the main disadvantage of the constant speed wind turbine, taking into account the DC-DC converter's dynamic performance that nullify the voltage fluctuation effect. Thus, VSWECS is preferred with maximum power tracking controllers connected with the voltage regulating DC-DC converter. Although DFIG based VSWECS is leading the market in the current era the size variation of the turbine by means of adding the gear box has led to the use of PMSG with more number of poles without gears. Since gearless PMSG is a VSWECS, the contribution of the power electronics devices is very high in maintaining a stable power delivery in the grid-connected system. Hence, it is essential to design and develop efficient control schemes on both machine side and grid side for direct driven variable speed wind turbine based on permanent magnet synchronous generator to regulate the voltage/frequency, active, reactive power, power factor, and total harmonics distortion

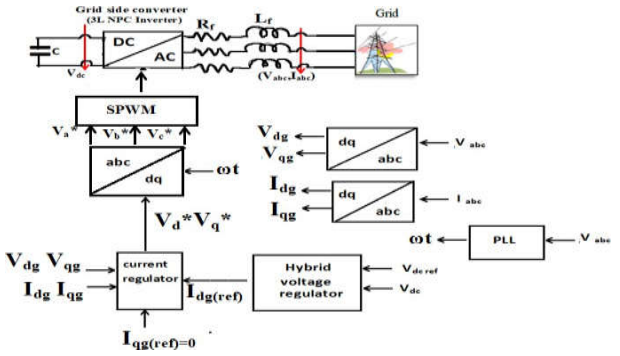

Figure 1. Flow diagram for grid side converter controller

The control of active and reactive power on the grid side is accomplished through a control technique that ensures the DC link voltage remains constant and adheres to the grid code specifications at the output of the grid-side converter. To enable independent control of both the generator-side and grid-side converters, a DC link capacitor isolates them.

Figure 1 depicts a hybrid vector control scheme for the grid-side converter. The GSC (Grid-Side Converter) Controller consists of several components, including:

1. Phase Locked Loop (PLL): The PLL is responsible for synchronizing the control system with the grid voltage, ensuring that the converter operates in phase with the grid.

2. Hybrid Voltage Regulator: This component manages the voltage control of the grid-side converter, ensuring that the DC link voltage remains constant within the desired range.

3. Current Regulator: The current regulator handles the control of grid-side current, allowing precise regulation of active and reactive power as needed.

This control scheme and its components work together to ensure that the grid-side converter operates efficiently, adheres to grid code requirements, and effectively manages active and reactive power flow in the system. The use of a DC link capacitor enables independent control of the generator-side and grid-side converters, enhancing the overall performance and stability of the system. The process involves measuring the grid terminal voltage Vabc and grid terminal current Iabc using current and voltage sensors. To determine the angle of the grid voltage, a Phase Locked Loop (PLL) is utilized, and its relationship with the angular frequency ω is described by Equation (33). The obtained ω value is used in either the abc to dq transformation or dq to abc transformation. Additionally, ω is determined using abc to αβ transformation. These transformations are fundamental in converting between different reference frames and simplifying the analysis and control of electrical systems. The PLL plays a crucial role in synchronizing the system with the grid voltage, ensuring accurate measurements and control actions.

$$\omega = \tan\left(\frac{V\beta}{V\alpha}\right) \quad (33)$$

In the given context, Vα and Vβ represent the two-phase αβ components of the grid voltage. These components are calculated using the equations provided in Equations (34 and 35). The transformation into αβ components is a common technique used to simplify the analysis and control of three-phase electrical systems, especially in applications like motor drives and power converters.

$$V_\alpha = \frac{2}{3}\left(V_{ag} - 0.5V_{bg} - 0.5V_{cg}\right) \quad (34)$$

$$V_\beta = \frac{2}{3}(0.866V_{bg} - 0.866V_{cg}) \quad (35)$$

Here, Vag, Vbg, and Vcg represent the abc components of the grid voltage, which are the instantaneous three-phase AC voltages. These components are mathematically represented by the equations provided in the range from Equation (36) to Equation (38). These equations describe the instantaneous values of the three-phase grid

voltages, which are essential for the analysis and control of electrical systems.

$$V_{ag} = V_p \sin(\omega_t) \quad (36)$$

$$V_{bg} = V_p \sin(\omega_t - 120^o) \quad (37)$$

$$V_{cg} = V_p \sin(\omega_t + 120^o) \quad (38)$$

Using the abc to dq conversion, the three-phase rotating voltage components Vag, Vbg, and Vcg are transformed into stationary components Vdg, Vqg, and Vo. This transformation is carried out in accordance with Equation (39). The abc to dq conversion is a mathematical technique that is frequently used in electrical engineering to simplify the analysis and control of three-phase systems. It allows for a more straightforward representation of the system's behavior in a reference frame that aligns with the rotor flux or other relevant quantities, making it easier to design and implement control strategies.

$$\begin{bmatrix} V_{dg} \\ V_{qg} \\ V_o \end{bmatrix} = \frac{3}{2} \begin{bmatrix} \sin\omega t & \sin(\omega t - 120^o) & \sin(\omega t + 120^o) \\ \cos\omega t & \cos(\omega t - 120^o) & \cos(\omega t + 120^o) \\ 0.5 & 0.5 & 0.5 \end{bmatrix} \begin{bmatrix} V_{ag} \\ V_{bg} \\ V_{cg} \end{bmatrix} \quad (39)$$

Similarly, using the abc to dq transformation, the three-phase current components Iag, Ibg, and Icg are converted into stationary components Idg, Iqg, and I0. This transformation is achieved in accordance with Equation (40). The abc to dq transformation is a common technique used to represent three-phase electrical quantities in a reference frame that simplifies control and analysis, particularly in systems like motor drives and inverters.

$$\begin{bmatrix} I_{dg} \\ I_{qg} \\ I_o \end{bmatrix} = \frac{3}{2} \begin{bmatrix} \sin\omega t & \sin(\omega t - 120^o) & \sin(\omega t + 120^o) \\ \cos\omega t & \cos(\omega t - 120^o) & \cos(\omega t + 120^o) \\ 0.5 & 0.5 & 0.5 \end{bmatrix} \begin{bmatrix} I_{ag} \\ I_{bg} \\ I_{cg} \end{bmatrix} \quad (40)$$

Figure 2 shows the abc coordinate and dq coordinate frames

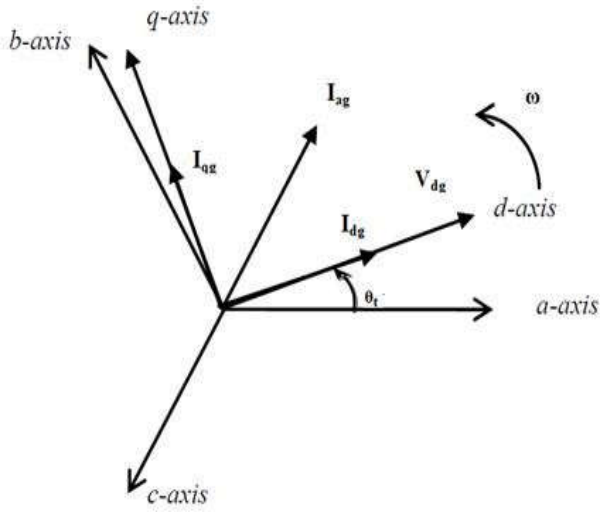

Figure 2. Time varying three phase abc to stationary dq frame transformation

Using dq coordinates the active and reactive power are represented by the Equations (41 and 42)

$$P_{grid} = 1.5(V_{dg}I_{dg} + V_{qg}I_{qg}) \quad (41)$$

$$Q_{grid} = 1.5(V_{qg}I_{dg} - V_{dg}I_{qg}) \quad (42)$$

As indicated in Equations (41) and (42), it's evident that both active and reactive power depend on both the direct (d) axis and quadrature (q) axis components. To achieve independent control of active and reactive power, it becomes necessary to implement a decoupling mechanism. This decoupling process separates the control of active power from that of reactive power, allowing for precise and independent regulation of these two important aspects of the system's performance.

In the context of dynamic decoupling, the goal is to set the quadrature axis voltage Vqg to zero by aligning the direct axis component with the voltage space vector, effectively ensuring that the quadrature axis component is always zero. When the reference frame is configured with Vqg=0, the active and reactive power can be expressed using Equations (43 and 44). This means that in this specific reference frame, the control focus is primarily on active power (P) and reactive power (Q), with Vqg being constrained to zero, simplifying the control objectives.

$$P_{grid} = 1.5V_{dg}I_{dg} \quad (43)$$

$$Q_{grid} = -1.5V_{dg}I_{qg} \quad (44)$$

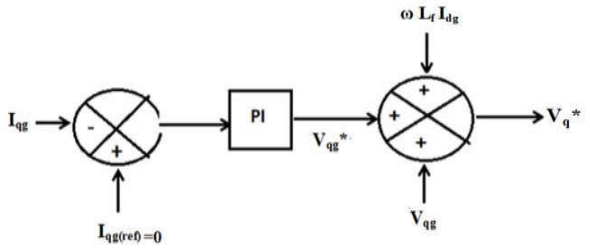

Figure 3. Flow diagram of d axis current regulator

Indeed, based on Equations (43) and (44), it becomes evident that for a given d-axis voltage value, the active and reactive powers can be controlled independently through the manipulation of the d-axis current component Idg and the q-axis current component Iqg, respectively. This capability allows for precise and separate control of both active and reactive power in the system, providing flexibility in meeting specific operational requirements and objectives. The d axis and q axis current regulator are shown in figure 3 and figure 4.

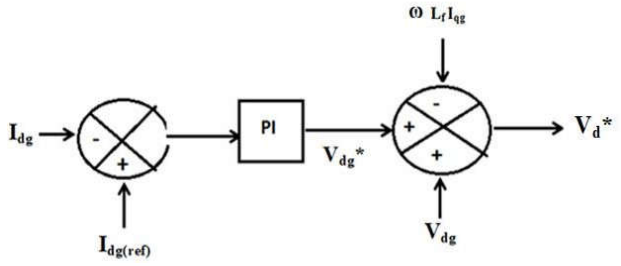

Figure 4. Flow diagram of q axis current regulator

The input to the PI controller or hybrid controller is the DC link voltage Vdc, which is measured and compared to the reference DC link voltage Vdc ref. The objective is to maintain a constant DC link voltage. In this control scheme, the q-axis reference current Iqg (ref) is intentionally set to zero to ensure that the power factor of the three-phase inverter remains unity.

Referring to Figure 3 and Figure 4, and neglecting the resistance in the grid-side line (Rf), the control equations in the dq coordinate system are given by Equations (3.63 and 3.64). These equations govern the control of the system in the dq reference frame, allowing for precise regulation of currents and voltages in the inverter.

$$V_d^* = V_{dg}^* - \omega_t I_{qg} L_f + V_{dg} \quad (45)$$

$$V_q^* = V_{qg}^* + \omega_t I_{dg} L_f + V_{qg} \quad (46)$$

Vdg* and Vqg* represent the reference voltage values for the d-axis and q-axis voltages, respectively. These values are determined using the equations provided in the text, specifically Equations (47 and 48). These reference voltage values play a crucial role in controlling the behavior of the system, particularly in maintaining desired characteristics in the d-q coordinate system.

$$V_{dg}^* = (Kp + \frac{Ki}{s})(I_{dg(ref)} - I_{dg}) \quad (47)$$

$$V_{qg}^* = (Kp + \frac{Ki}{s})(I_{qg(ref)} - I_{qg}) \quad (48)$$

The Vd* and Vq* components are further processed by converting them into three-phase time-varying AC components using a dq to abc transformation, as described by Equation (49). This transformation allows for the representation of these components in the three-phase reference frame, making them suitable for use in three-phase systems.

$$\begin{bmatrix} V_a^* \\ V_b^* \\ V_c^* \end{bmatrix} = \begin{bmatrix} \sin(\omega t) & \cos(\omega t) & 1 \\ \sin(\omega t - 120^\circ) & \cos(\omega t - 120^\circ) & 1 \\ \sin(\omega t + 120^\circ) & \cos(\omega t + 120^\circ) & 1 \end{bmatrix} \begin{bmatrix} V_d^* \\ V_q^* \\ 0 \end{bmatrix} \quad (49)$$

The process involves comparing the reference signals Va*, Vb*, and Vc* with triangular wave carrier signals within the Pulse Width Modulation (PWM) controller. The PWM controller then generates gate signals based on this comparison. These gate signals are subsequently employed to trigger the switches within the three-phase inverter, controlling the output voltage and current to meet the desired reference values Va*, Vb*, and Vc*. This technique is commonly used in power electronics for voltage and current control in three-phase systems.

PI Controller

To model a PI (Proportional-Integral) controller, you can use a transfer function representation. The transfer function describes the relationship between the controller input (error signal) and the controller output (control signal). The transfer function of a PI controller is given by:

$$C(s) = Kp + Ki/s \quad (50)$$

Where:

- C(s) is the Laplace transform of the controller output.

- Kp is the proportional gain, which determines the strength of the proportional control action.

- Ki is the integral gain, which determines the strength of the integral control action.

- s is the complex frequency variable.

The term Kp represents the proportional control action and is responsible for responding to the instantaneous error. It produces a control output that is proportional to the error signal. The term Ki/s represents the integral control action. The integral of the error over time is accumulated and multiplied by the integral gain Ki. It helps eliminate steady-state error and allows the controller to respond to constant or slowly changing errors. To use the transfer function representation, you can apply it in a control system block diagram. The error signal (the difference between the setpoint and the process variable) is fed into the PI controller, and the

controller output is used to actuate the process or system being controlled. Keep in mind that the specific values of Kp and Ki need to be carefully selected and tuned for a given control application. Different tuning methods, such as Ziegler-Nichols or trial and error, can be used to determine suitable values for achieving desired control performance, such as stability, responsiveness, and accuracy.

(FLC) is appropriate for systems that are hard to manipulate. mainly due to the existing nonlinear complexities. This is because, unlike a conventional PI controller, rigorous mathematical formulation is not needed to design a good fuzzy controller. The database which comprises of membership functions lies between 0 and 1. The main processes in FLC are fuzzification, interference mechanism and defuzzification. The interference method uses a set of linguistic rules to convert the input conditions into a fuzzified output. Finally, defuzzification is used to convert the fuzzy outputs into required data. The block diagram for fuzzy logic based current regulation is shown in Figure 5. The fuzzy logic rules are developed by absorbing the characteristic of the PI controller and PID controller performances.

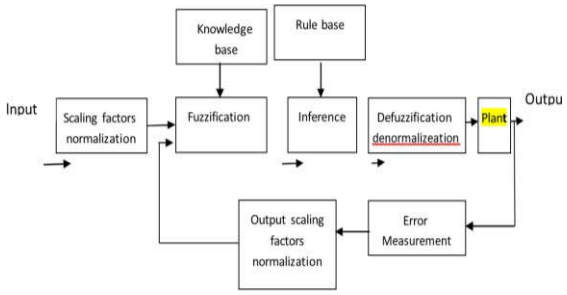

Figure 5. Fuzzy controller block diagram

(FLC) is appropriate (FLC) is appropriate for systems that are hard to manipulate. mainly due to the existing nonlinear complexities. Fuzzification is an essential aspect in fuzzy logic theory. Fuzzification is the process in which the crisp values are converted to fuzzy. By identifying certain uncertainties present in the crisp values, the fuzzy values have been formulated. The conversion of fuzzy values is denoted by the membership function.

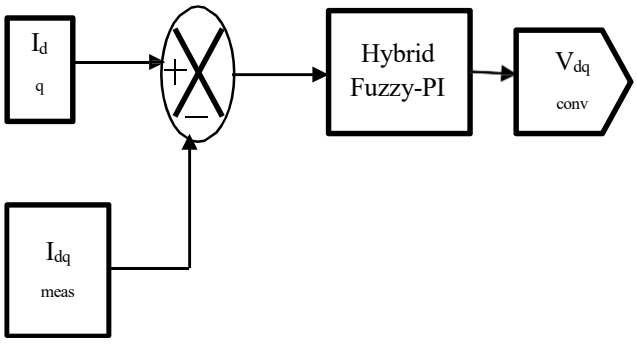

Figure 6. Hybrid Fuzzy-PI controller

err \ ce	Low	Medium	High
Low	Low	High	Medium
Medium	Low	High	High
High	Medium	Low	Medium

Table 1. Current Controller Fuzzy Logic Rules

The Table 1 and figure shows the rules of the Fuzzy logic inference system and developed based on input and output parameters of FLC. The supplementary type of hybrid controller is where both PI and FLC contributes to the reference voltage. Fuzzification is the process in which the crisp values are converted to fuzzy. By identifying certain uncertainties present in the crisp values, the fuzzy values have been formulated. The conversion of fuzzy values is denoted by the membership function. Defuzzification results in the fuzzy to crisp conversions. The fuzzy results generated cannot be used as such to the applications, hence it is necessary to convert the fuzzy quantities into crisp quantities for further processing.

FLC Design Methodology

The fuzzy results generated cannot be used as such to the applications, hence it is necessary to convert the fuzzy quantities into crisp quantities for further processing. The design of the FLC comprises of the following steps,

Membership functions

The fuzzy results generated cannot be used as such to the applications, hence it is necessary to convert the fuzzy quantities into crisp quantities for further processing. In fuzzy set theory, a membership function defines the degree of a crisp value in a range between 0 and 1. This helps in designing the systems with uncertainty or ill-defined problems in read world. Membership function is a function which returns membership degree of how a crisp value is mapped to an input space. Each membership function contains a curve which represents each point in a specified input partition. In FLC, the type of membership function used in the present work is triangular membership function.as it is the simplest shape among the other type of membership functions such as bell shaped, trapezoidal and Gaussian membership functions. The number of membership function determines the quality of control which can be achieved using FLC. As the number of membership function increases, the quality of the controller improves at the cost of increased computational time and memory.

Inference Engine

After fixing the input and the output for the Fuzzy logic training using the membership functions a group of rules are written to connect the input and the output membership functions. The rules are written in terms of if then rules. The collection of these rules is called the inference engine. While the inference engine is made ready the FLC is ready for working.

The analysis of power quality in the solar photovoltaic model is taken for the proposed work. The system of the solar photovoltaic panel is integrated with the power grid. Solutions for power quality issues in the distributed network is solved by means of traditional and intelligent techniques in the research thus carried out. The power quality improvement

with traditional converters like the PI controller and the adaptive PI controllers are carried out to distinguish the performance evaluation. Traditional PI controller adopting the manual tuning method and the advanced controller using the adaptive tuning method that tunes the gain parameters of the PI controllers using the controller and the supplementary Fuzzy- PI hybrid controller.

The implementation of the Fuzzy PI implementation needs a parallel FLC with the PI controller which provides a cumulative output. This hybrid controller is called supplementary controller that actually uses both the Fuzzy and the PI controller output to get the reference voltage for the PWM controller.

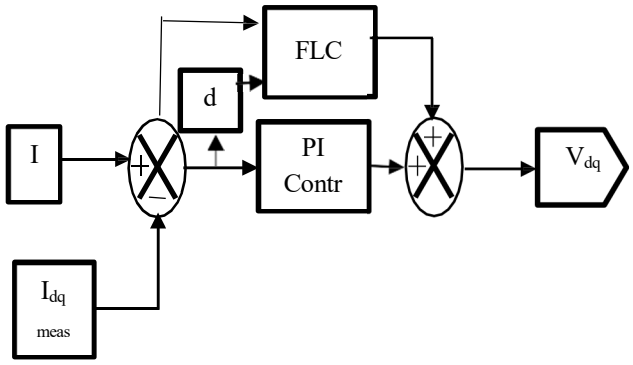

Figure: 7 Supplementary Fuzzy Controller based Current Regulator

The supplementary Fuzzy PI controller or the hybrid Fuzzy-PI method produces the output from both the Fuzzy controller and the PI controller. The weightage of both the controllers are equally taken for the output reference voltage and cumulated.

The error and change in error in the dq domain are used as the input to the FLC to generate the output values from the inference engine and the PI controller also produces the output.

Component	Specification
Wind Turbine	
Mechanical Power	20 kW
Wind Speed	12 m/s
Torque	6 Nm
PMSG	
Back EMF	Sinusoidal
Rotor Type	Salient pole
Pole Pairs	4
Torque	6 Nm
Boost Converter	
Inductor	5 mH
Capacitor	12000 μF
Switching Frequency	50 kHz
DC Link and Inverter	
Vdc (DC Link Voltage)	300 Volts
Inverter output voltage	440 V
Inductive filter	2 mH
Transformer	
kVA Rating	100
Low Side Voltage	415V
High Side Voltage	11 kV
Frequency	50 Hz
Grid	
MVA Rating	100
Voltage	11 kV
Frequency	50 Hz
Power	100 kW
Frequency	50 Hz

Table 2. Parameters of the components used in the proposed AC-DC-AC converter

MATLAB based implementation is developed for the comparative analysis of the six phase generator connected to the grid with both the traditional PI controller and the Hybrid controllers like parallel and series PI-Fuzzy controllers. The grid integration from the WECS is through the inverter. The parameters chosen for the simulation is as given in the Table 2. The implementation of the Wind Energy Conversion System (WECS) with an AC-DC-AC power conversion unit is carried out using the SimPowerSystems toolbox in MATLAB/Simulink software. The MATLAB model incorporates a wind turbine with a Permanent Magnet Synchronous Generator (PMSG) designed with the following specifications: rated voltage of 300 V, rated speed of 4500 rpm, and a power output of 20 kW. To mitigate the transients originating from the generator, an LC filter is employed between the rectifier and the generator. The LC filter consists of an inductor, denoted as Lf, with a value of 3 mH, and a capacitor, denoted as Cf, with a value of 2 μF. This LC filter configuration is chosen to effectively reduce the undesired transients and maintain a smoother output from the generator. By utilizing the SimPowerSystems toolbox in MATLAB, we can simulate the dynamic behavior of the WECS and assess its performance under various operating conditions. The implemented model allows for the evaluation of the system's response to changes in wind speed, load variations, and grid disturbances, providing insights into the behavior and effectiveness of the proposed control strategy. The utilization of MATLAB/Simulink and the SimPowerSystems toolbox offers a comprehensive platform for the investigation and analysis of the FUZZY controller's performance in the context of the WECS with AC-DC-AC power conversion unit and the specific PMSG generator model. The simulations conducted using this setup provide valuable data for assessing the controller's effectiveness in regulating power output, voltage stability, and disturbance rejection. Throughout the subsequent sections, the simulation setup and methodology will be described in detail, allowing for a thorough investigation and analysis of the Fuzzy controller's performance in the considered WECS configuration with the specified PMSG generator model.

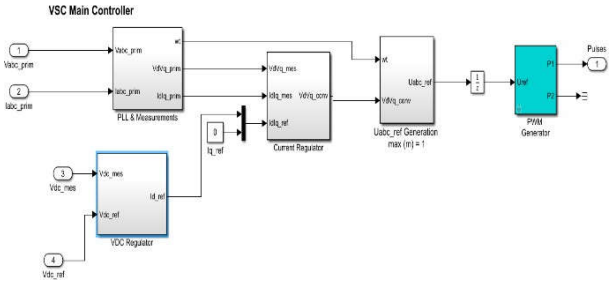

Figure 8. Simulink model of the proposed system

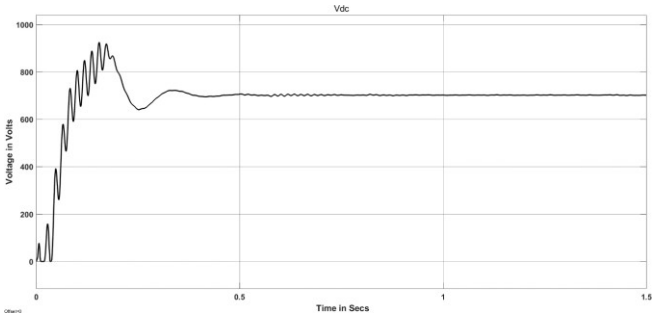

Figure 9. SPMSG Output at its Six-Phase Terminal

In this study, an alternative intelligent control loop is implemented by replacing the existing control loop with a Fuzzy controller. The Fuzzy controller is implemented using the corresponding block sets available in MATLAB. This intelligent control loop aims to improve the performance of the system compared to the conventional control loop. By incorporating the Fuzzy controller into the control scheme, we expect to achieve enhanced control accuracy, robustness, and stability. The Fuzzy controller's characteristics enable better adaptation to the nonlinear dynamics and uncertainties of the system, leading to improved control performance. The performance improvement resulting from the conversion to intelligent control loops, specifically the Fuzzy controller, will be thoroughly discussed in the later part of this chapter. The analysis will focus on evaluating various performance metrics, such as power tracking, voltage regulation, and disturbance rejection. By comparing the results obtained with the Fuzzy controller to those achieved with the conventional control loop, we can assess the effectiveness of the intelligent control approach. Furthermore, the discussion will explore the advantages and limitations of the Fuzzy controller in the context of the considered WECS configuration. This analysis will provide valuable insights into the potential benefits of incorporating intelligent control techniques in the control strategy of grid-connected WECS with Six-Phase PMSG. `Overall, the implementation of the Fuzzy controller as an intelligent control loop presents an opportunity to evaluate the performance improvement achieved by adopting advanced control techniques. The subsequent discussion will delve into the analysis and interpretation of the simulation results, providing a comprehensive understanding of the benefits and implications of utilizing intelligent control loops in grid-connected WECS.

In the wind power simulation, a six-phase PMSG and rectifier bridge are used. The DC output is regulated by a DC-DC converter with MPPT, and then converted back to AC using a converter with DQ control. Figure 5.2 shows the generator voltage response to a variable wind speed. Nonlinear characteristics of the rectifier cause voltage distortion, leading to harmonics and torque ripples. However, suitable control techniques maintain a power factor close to unity for the SPMSG

The fulfillment of the grid code requirements at the Point of Common Coupling (PCC) is achieved through the Utilization of the Grid-Side Converter (GSC) and the dq (PI) controller. In the proposed model, the Generator-Side Converter (GSC) employs a three-phase bridge rectifier. As the wind speed fluctuates, the output DC voltage at the DC link experiences variations, as illustrated in Figure 5.3. By implementing appropriate control strategies, such as the dq (Fuzzy) controller, the proposed model aims to regulate the DC voltage at the link and ensure compliance with the grid code requirements. The dq (Fuzzy) controller utilizes the GSC to achieve this objective by adjusting the converter-controlled pulses based on the AC power conditions, enabling effective regulation of the generated power. Figure 9 provides a visual representation of the changes observed in the output DC voltage at the DC link in response to variations in wind speed. The fluctuations in wind speed impact the power generated by the wind turbine, leading to corresponding changes in the DC voltage level. Analyzing and understanding these voltage variations is crucial for assessing the performance of the control system and evaluating its ability to maintain stable operation and adhere to the grid code requirements.

The Boosted DC Voltage refers to the voltage level obtained after implementing the (MPPT) algorithm, specifically the Incremental Conductance algorithm, in a wind power generation system. In the context of the Boosted DC Voltage, the MPPT algorithm tracks the maximum power point of the wind turbine by dynamically adjusting the DC-DC converter's duty cycle. The algorithm compares the instantaneous power output of the wind turbine with its derivative, or the rate of change of power with respect to the generator speed. By comparing these values, the algorithm can determine the direction to adjust the duty cycle for maximizing power output. This voltage level ensures that the wind turbine operates at its maximum power point, allowing for efficient energy conversion and power extraction from the wind source.

The figure 10 illustrates the grid voltage and current waveforms after connecting the Synchronous Permanent Magnet Synchronous Generator (SPMSG) to the grid using a controller at the grid side. When integrating a SPMSG into the grid, it is crucial to regulate the generated power and ensure the compatibility of the SPMSG's output with the grid requirements. The FUZZY controller is employed in this scenario to achieve precise control of the grid-side converter and maintain the desired grid voltage and current

Characteristics. The grid voltage waveform indicates the electrical potential difference supplied by the grid, while the grid current waveform represents the electrical current flowing between the SPMSG and the grid. These waveforms exhibit the behavior of the grid variables when the SPMSG is connected and controlled by the FUZZY controller. By utilizing the FUZZY controller, the grid voltage and current can be regulated effectively. The FUZZY controller leverages the characteristics to address the nonlinear dynamics and uncertainties of the system, providing improved control accuracy, stability, and robustness. Analyzing the grid voltage and current waveforms allows us to assess the performance of the FUZZY controller in maintaining the desired grid conditions. It provides insights into how well the controller regulates the power flow and ensures the stability and quality of the grid-connected SPMSG system. Understanding and optimizing the behavior of the grid voltage and current through the FUZZY controller is crucial for ensuring the reliable and efficient operation of the SPMSG-based wind power generation system.

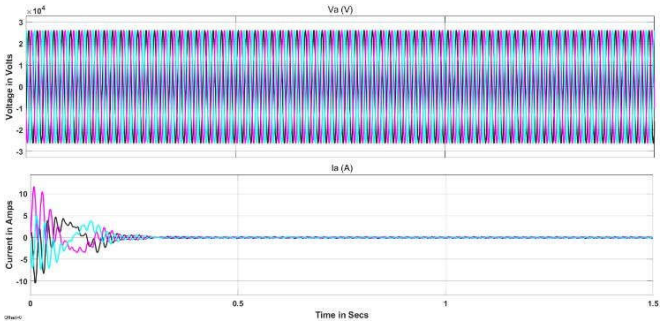

Figure 10. Grid Voltage and Current after Connecting SPMSG

The implementation of control techniques at each conversion stage in the wind power generation system allows for the extraction of useful power on the generator side. This leads to a decrease in the presence of harmonics at the source side. The FFT analysis allows us to examine the frequency components present in the signals and assess the level of harmonics. The generator operates at a frequency determined by its 4 pole pairs, corresponding to a speed of 3600 RPM, resulting in a frequency of 120 Hz.

Figure 11 represents the real and reactive power at the grid when employing the Fuzzy controller. This figure provides valuable insights into the power flow and characteristics of the grid-connected system.

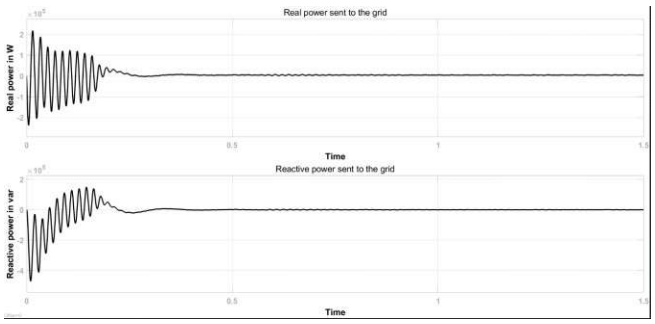

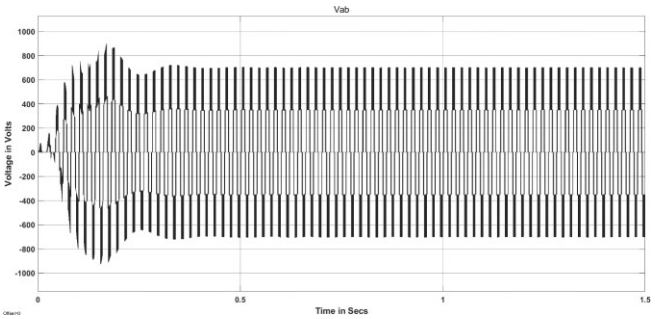

Figure 11. Real and Reactive Power at the Grid using FUZZY controller

The Fuzzy controller is implemented to regulate the real and reactive power at the grid. By controlling the converter and adjusting the power flow, the FUZZY controller ensures that the system operates at the desired power levels and meets the grid requirements. Analyzing Figure 10 and 11 allows us to assess the performance of the Fuzzy controller in maintaining the real and reactive power within the desired limits. By observing the variations in the real and reactive power waveforms, we can determine how effectively the controller responds to changes in the system and grid conditions. A well-designed FUZZY controller should enable accurate tracking and control of the real and reactive power, minimizing deviations and maintaining stability in the grid-connected system. The FUZZY controller's characteristics provide enhanced adaptability to the nonlinear dynamics and uncertainties of the system, ensuring improved control accuracy, robustness, and stability.

Figure 5.10 presents a comparison of the real power profiles obtained using three different controllers: (PI), (), and (FUZZY). This figure allows for a comprehensive evaluation of the performance of each controller in terms of real power regulation over the entire simulation duration. Figure 5.11 provides a zoomed-in view of the real power comparison specifically within the time interval of 0 to 0.2 seconds. This detailed view allows for a closer examination of the controllers' performance during the initial transient period, capturing their response to sudden changes and their ability to stabilize the real power output. Figure 5.12 offers a zoomed view of the real power comparison in the time interval of 0.2 to 0.6 seconds. This focused analysis provides insights into the controllers' performance during a specific period, revealing any discrepancies in power regulation and the controllers' ability to maintain stability over an extended duration.

The chapter focused on the investigation and analysis of the FUZZY controller for grid-connected (WECS) with Six-Phase Permanent Magnet Synchronous Generator (PMSG). The objective was to evaluate the effectiveness of this advanced control strategy in regulating power output and ensuring system stability. By utilizing the adaptive and self-tuning capabilities of the and the of the FUZZY controller, improved control accuracy, robustness, and stability can be achieved for Six-Phase PMSG-based WECS. This is crucial

Considering the nonlinear dynamics and uncertainties associated with these systems. Through simulation studies, the performance of the FUZZY controller was evaluated in terms of power tracking, voltage regulation, and disturbance rejection under various operating conditions and system uncertainties. The controller's performance was compared to traditional control techniques, such as the PI controller, to highlight its superiority in addressing the challenges specific to Six-Phase PMSG-based WECS. Overall, this investigation contributes to the advancement of control techniques for efficient and reliable renewable energy systems. The FUZZY controller shows promise in enhancing the performance of grid-connected WECS, leading to increased power generation, improved stability, and reduced reliance on conventional energy sources.

Component	Specification
Wind Turbine	
Mechanical Power	20 kW
Wind Speed	12 m/s
Torque	6 Nm
PMSG	
Back EMF	Sinusoidal
Rotor Type	Salient pole
Pole Pairs	4
Torque	6 Nm
Boost Converter	
Inductor	5 mH
Capacitor	12000 μF
Switching Frequency	50 kHz
DC Link and Inverter	
Vdc (DC Link Voltage)	300 Volts
Inverter output voltage	440 V
Inductive filter	2 mH
Transformer	
kVA Rating	100
Low Side Voltage	415V
High Side Voltage	11 kV
Frequency	50 Hz
Grid	
MVA Rating	100
Voltage	11 kV
Frequency	50 Hz
Power	100 kW
Frequency	50 Hz

Table 3. Parameters of the components used in the proposed AC-DC-AC converter

REFERENCES

[1] Jabir M, Azil Illias, H, Raza S, Mokhlis, H, 'Intermittent smoothing approaches for wind power output:A review', Energies, vol. 10, pp. 1572-1577, 2017.

[2] Mohod S W, Aware, M V, 'A STATCOM-control scheme for grid connected wind energy system for power quality improvement', IEEE System Journal, vol. 4, pp. 346–352, 2010.

[3] Thiringer T, Petru T, Liljegren C, 'Power quality impact of a sea located hybrid wind park', IEEE Transaction on Energy Conversion, vol. 16, pp. 123–127, 2001.

[4] Mohamed M A, Eltamaly A M, Alolah A I, 'PSO-based smart grid application for sizing and optimization of hybrid renewable energy systems', PLoS ONE, 2016.

[5] Chen Z, Spooner E, 'Grid power quality with variable speed wind turbines', IEEE Trans. Energy Convers, vol 16, pp. 148–154, 2001.

[6] British Standards Institution. BS EN 50160: Voltage Characteristics of Electricity Supplied by Public Distribution Networks; British Standards Institution: London, UK, 2007.

[7] International Standard. Measurement and Assessment of Power Quality Characteristics of Grid Connected Wind Turbines; IEC 61400-21; CIE/IEC: Geneva, Switzerland, 2001.

[8] Nassif A B, Xu W, 'Passive harmonic filters for medium-voltage industrial systems: Practical considerations and topology analysis', In Proceedings of the 2007 39th North American Power Symposium, Las Cruces, NM, USA, pp. 301–307, 30 September–2 October 2007.

[9] Salam Z, Tan P C, Jusoh A, 'Harmonics mitigation using active power filter: A technological review', Electrical Journal of Engineering, vol. 8, pp. 17–26, 2006.

[10] Das J, 'Passive filters-potentialities and limitations', IEEE Transaction on Industrial Applications, vol. 40, pp. 232–241, 2004.

[11] Saeed Golestan, Josep M, Guerrero, Juan C, Vasquez, 'Single- Phase PLLs: A Review of Recent Advances', IEEE Transaction on Power Electronics, vol. 32, no. 12, pp. 9013-9030, 2017.

[12] M. Karimi-Ghartemani, S A Khajehoddin, P K Jain, A Bakhshai, 'Problems of startup and phase jumps in PLL systems', IEEE Transaction on Power Electronics, vol. 27, no. 4, pp. 1830-1838, 2012.

[13] S Golestan, M Ramezani, J M Guerrero, F D Freijedo, M Monfared, 'Moving average filter based phase-locked loops: Performance analysis and design guidelines', IEEE Transaction on Power Electronics, vol. 29, no. 6, pp. 2750-2763, 2014.

[14] Zunaib Alia, Nicholas Christofidesa, Lenos Hadjidemetrioub, Elias Kyriakidesb, Yongheng Yangc, Frede Blaabjergc, 'Three-Phase Phase- Locked Loop Synchronization Algorithms for Grid-Connected Renewable Energy Systems: A Review', Renewable and Sustainable Energy Reviews, vol. 90, pp. 434-452, 2018.

[15] Vineet P, Chandranh, Shadab Murshid, Bhim Singh, 'Power Quality Improvement for PMSG Based Isolated Small Hydro System Feeding Three-Phase 4-Wire Unbalanced Nonlinear Loads', 2019 IEEE Transportation Electrification Conference and Expo (ITEC), Detroit, USA, 2019.

[16] Md Shamim Reza, Mihai Ciobotaru, Vassilios G Agelidis, 'Grid Voltage Offset and Harmonics Rejection Using Second Order Generalized Integrator and Kalman Filter Technique', IEEE 7th International Power Electronics and Motion Control Conference, Harbin, China, pp. 104-111, 2012.

[17] Pedro Rodriguez, Alvaro Luna, Raul Santiago, Munoz-Aguilar, 'A Stationary Reference Frame Grid Synchronization System for Three-Phase Grid-Connected Power Converters Under Adverse Grid Conditions', IEEE Transaction on Power Electronics, vol. 27, no. 1, pp. 99-112, 2012.

[18] Harrag A & Messalti S, 'Variable step size modified P&O MPPT algorithm using GA-based hybrid offline/online PID controller', Renewable and Sustainable Energy Reviews, vol. 49, pp. 1247-1260, 2015.

[19] Linus RM & Damodharan P, 'Maximum power point tracking method using a modified perturb and observe algorithm for grid connected wind energy conversion systems', IET Renewable Power Generation, vol. 9, no. 6, pp. 682-689, 2015.

[20] Fesharaki VJ, Sheikholeslam F & Jahed Motlagh MR, 'Maximum power point tracking with constraint feedback linearization controller and modified incremental conductance algorithm', Transactions of the Institute of Measurement and Control, vol. 40, no. 7, pp. 2322-2331, 2018.

[21] Giannakis A, Karlis A & Karnavas YL, 'A combined control strategy of a DFIG based on a sensorless power control through modified phase-locked loop and fuzzy logic controllers', Renewable energy, vol. 121, pp. 489-501, 2018.

[22] Asghar AB & Liu X, 'Adaptive neuro-fuzzy algorithm to estimate effective wind speed and optimal rotor speed for variable-speed wind turbine', Neurocomputing, vol. 272, pp. 495-504, 2018.

[23] Deepak Pullaguram, Sukumar Mishra, Nilanjan Senroy, Monish Mukherjee, 'Design and tuning of robust fractional order controller for autonomous microgrid VSC system', IEEE Transaction on Industry Applications, vol. 54, no. 1, pp, 91-101, 2018.

[24] Beddar Antar, Bouzekri Hassen, Badreddine Babes, Hamza Afghoul, 'Fractional order PI controller for grid connected wind energy conversion system', 2015 4th International Conference on Electrical Engineering (ICEE), Boumerdes, Algeria, 2015.

[25] C Vivierors, R Melicio, J M Igreja, V M F Mendes, 'Fuzzy, Integer and Fractional-Order control application on a wind turbine benchmark

model', 19th International Conference on Methods and Models in Automation and Robotics (MMAR), pp. 252-257, Poland, 2014.

[26] Y Soufi, S Kahla, M Bechouat, 'Particle Swarm Optimization Based Sliding Mode Control of Variable Speed Wind Energy Conversion System', International Journal of Hydrogen Energy, vol. 41, no. 45, pp. 20956-20963, 2016.

[27] Mao Jingfeng, Wu Aihua, Wu Guoqing, Zhang Xudong, 'Maximum power point tracking in variable speed wind turbine system via optimal torque sliding mode control strategy', 34th Chinese Control Conference (CCC), pp.7967-7971, China, 2015.

[28] L Sidhom, I Chihi, S Sahraoui, A Abdelkrim, 'Intelligent-PI controller for electro-hydraulic system', 4th International Conference on Control Engineering and Information Technology (CEIT), Tunisia, 2016.

[29] T Agee, Selcuk Kizir, Zafer Bingul, 'Intelligent proportional- integral (iPI) control of a single link flexible joint manipulator', Journal of Vibration and Control, vol. 21, no. 11, pp. 2273-228, 2015.

[30] Radu-Emil Precup, Mircea-Bogdan Radac, Raul-Cristian Roman, Emil M. Petriu, 'Model-free sliding mode control of nonlinear systems: Algorithms and experiments', Information Sciences, Elsevier, vol. 381, pp. 176-192, 2017.

[31] Rachid Errouissi, Ahmed Al-Durra, 'A Novel PI type Sliding Surface for PMSG-based wind turbine with improved transient performance', IEEE Transaction on Energy Conversion, vol. 33, no. 2, pp. 834-844, 2018.

[32] Yoon-Cheul Jeung, Dong-Choon Lee, 'Voltage and Current Regulation of Bi-directional Isolated Dual Active Bridge DC-DC Converters based on Double-Integral Sliding Mode Control', IEEE Transaction on Power Electronics, vol. 34, no. 7, pp. 6937-6946, 2019.

[33] Y Feng, X Yu, Z Man, 'Non-singular terminal sliding mode control of rigid manipulators', Automatica, vol. 38, no. 12, pp. 2159-2167, 2002.

[34] Kaihui Zhao, Tonghuan Yin, Changfan Zhang, Jing He, Xiangfei Li, Yue Chen, Ruirui Zhou, Aojie Leng, 'Robust Model-Free Nonsingular Terminal Sliding Mode Control for PMSM Demagnetization Fault', IEEE ACCESS, vol. 7, 2019.

[35] Mohammad Javad Morshed, Afef Fekih, 'A Sliding Mode Approach to Enhance the Power Quality of Wind Turbines Under Unbalanced Voltage Conditions', IEEE/CAA Journal of Automatica Sinica, vol. 6, no. 2, pp. 566-574, 2019.

[36] Zhenxin He, Chuntong Liu, Ying Zhan, Hongcai Li, Xianxiang Huang, Zhili Zhang, 'Nonsingular Fast Terminal Sliding Mode Control with Extended State Observer and Tracking Differentiator for Uncertain Nonlinear Systems', Hindawi Publishing Corporation, Mathematical Problems in Engineering, vol. 2, pp. 1-17, 2014.

[37] Schiferl RF, 'Six phase synchronous machine with ac and dc stator connections, Part I: Equivalent circuit representation & steadystate analysis', IEEE transactions on power apparatus and systems in 1983. Schiferl RF, 'Six phase synchronous machine with ac and dc stator connections, Part II: Harmonic studies and a proposed uninterruptible power supply scheme', IEEE transactions on power apparatus and systems in 1983.

[38] Sudhoff SD, 'Analysis and average-value modeling of dual line-commutated converter 6phase synchronous machine systems', IEEE transactions on energy conversion in 1993.

[39] Nataraja. C, Dr G S Sheshadri, 'A Proposed Methodology for Intelligent Control of Six Phase PMSG in a Grid Connected Wind Energy Conversion System', International Journal for Research in Applied Science & Engineering Technology (IJRASET) ISSN: 2321-9653; vol. 9, Issue 7, July 2021.

[40] Nataraja. C, Dr G S Sheshadri, 'Grid Connected PI controller of SPMSG in WECS', SSAHE-Journal of Interdisciplinary Research, ISSN: 2582-9890; Vol. 2, Issue 2, pp. 21-31, June 2022.

[41] Concordia C, de-Mello F P, 'Concepts of synchronous machine stability as affected by excitation control. IEEE transactions on power apparatus system', PAS, vol. 88, pp. 316- 329, 1969.

[42] Alizadeh M, Kojori S S, Ganjefar S, 'A modular neural block to enhance power system stability', IEEE transactions on power systems, vol. 28, no. 4, pp. 4849-4856, 2013.

[43] Darabian M, Jalilvand A, 'A power control strategy to improve power system stability in the presence of wind farms using FACTS devices and predictive control'. Electrical power energy system, vol. 85, pp. 50-66, 2017.

[44] HsuI C F, Lee T T, Tanaka K, 'Intelligent non-singular terminal sliding-mode control via perturbed fuzzy neural network', Engineering applications of artificial intelligence, vol. 45, pp. 339–349, 2015.

[45] Segal R, Sharma A, Kothari M L, ' A self- tuning power system stabilizer based on artificial neural network', Electrical power & energy systems, vol. 26, no. 6, pp. 423–30, 2004.D. Jovcic, “Series LC DC circuit breaker,” *High Volt.*, vol. 4, no. 2, pp. 130–137, Jun. 2019, doi: 10.1049/hve.2019.0003.